A CAD Method for Centrifugal Compressor Impellers

H. Krain
Research Engineer, DFVLR,
Institut fur Antriebstechnik,
Cologne, West Germany

A computer-aided design method (CAD) has been developed for radially ending and backswept centrifugal compressor impellers. The geometrical concept introduced for generating the impeller geometry takes care of numerical, manufacturing, as well as aerodynamic aspects. The fluid dynamic calculation method applied is based on a quasi-three-dimensional approach coupled with a boundary layer calculation method. Detailed quantitative comparisons between theoretical data and laser measurements taken within a radially ending impeller revealed predominantly good agreement. Backswept impellers of different size and shape have been designed by the approach presented.

Introduction

Surge and efficiency of centrifugal compressors are known to be significantly influenced by the impeller discharge flow characteristics. Generally, a highly distorted, unsteady jet/wake pattern is expected within the impeller exit/diffuser inlet area, which additionally complicates a reliable prediction of throat blockage and channel diffuser recovery [1, 2, 3]. Extensive laser measurements carried out at DFVLR, Cologne, revealed strong effects of the separated impeller discharge flow on the vaned diffuser inlet conditions [1]. Unsteady flow angle fluctuations up to 17 deg superimposed by a considerable flow angle difference between hub and shroud have been analyzed within the vaned diffuser inlet area. Furthermore, noticeable impeller reactions occured even far downstream of the diffuser throat where usually steady-state conditions are presumed [4]. In this area unsteady flow angle fluctuations up to 10 deg were still present, proving that a channel diffuser design based on a steady-state approach is doubtful, as far as the diffuser is coupled with a heavily separated impeller [3, 5, 17]. Therefore, a steady impeller discharge flow is desirable not only in regard to flow range and efficiency improvements but also with respect to a reliable and simplified diffuser design.

Aiming at this goal, today's advanced aerodynamic calculation methods should become quick and reliable impeller design tools capable of generating smooth impeller discharge flows. But, due to the three-dimensional flow effects, such theories are difficult to apply in the centrifugal compressor aerodynamics. Nevertheless, significant improvements have been obtained during the last years [6, 7, 8, 9]. Presently, even three-dimensional viscous theories are treated, and reasonable results have been presented [10, 11]. However, since an impelller design optimization generally is an iterative process, storage and central processor unit time are important quantities even in view of high-speed digital computers. Additionally, a simple input data preparation as well as an easily understandable output preparation are necessary for such a design approach. Last but not least, the design procedure should withstand a quantitative check with reliable measurements taken within centrifugal compressor impellers running under realistic operating conditions. An impeller design method meeting the requirements indicated has been developed at DFVLR.

Design Approach

A block diagram illustrating the design procedure is shown in Fig. 1. The overall design package has a modular structure, thus ensuring a time efficient operation. Initially, the impeller geometry is generated and the geometrical quantities necessary for the fluid dynamic calculation are prepared. Based on Wu's streamsheet approach [12] the fluid dynamic quantities are calculated on hub-to-shroud and blade-to-blade stream surfaces introduced to simplify the three-dimensional flow problem. In addition, a boundary layer calculation is involved providing information on the tolerable deceleration of the relative flow [13]. The results obtained may be analyzed

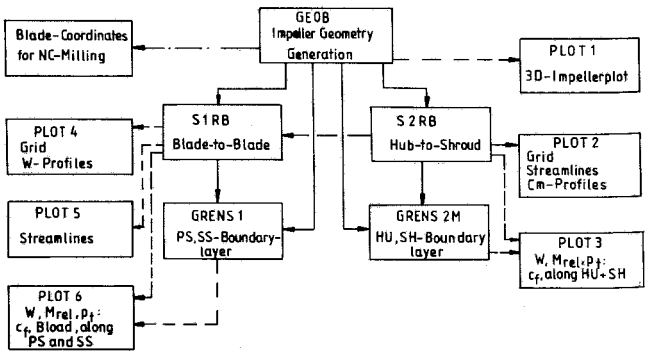

Fig. 1 Block diagram of the impeller design procedure

Contributed by the Gas Turbine Division of THE AMERICAN SOCIETY OF MECHANICAL ENGINEERS and presented at the 28th International Gas Turbine Conference and Exhibit, Phoenix, Arizona, March 27–31, 1983. Manuscript received at ASME Headquarters December 21, 1981. Paper No. 83-GT-65.

on a graphic terminal by means of the six plot-modules available. Figure 1 displays a coupling between the hub-to-shroud and blade-to-blade solution. The blade-to-blade calculation can be carried out independently for different radial positions. The input data for these calculations are prepared by the geometrical program (GEOB) as well as by the hub-to-shroud solution (S2RB). Thus the results obtained by the blade-to-blade calculations are directly dependent on the hub-to-shroud solution; reactions of the blade-to-blade solutions on the hub-to-shroud solution are neglected. Similarly, a direct interaction between the boundary layer calculation and the flow field solutions have not yet been taken into account, because this would only be an appropriate approach if an unseparated flow could be ensured during the whole iterative design process. Thus the results of the boundary layer calculations are primarily taken as a criterion for flow stability. Additionally, the local displacement thickness is taken from these results to account for the aerodynamic blockage during the final design. The input for the plot-modules (PLOT2 ÷ PLOT6) is taken from the flow field and boundary layer calculations. The grids used for the flow field calculations as well as the velocity, Mach number, and total pressure distributions are plotted. These quantities are results of the flow field calculations. Additionally, the skin friction coefficient, c_f, which is a result of the boundary layer calculation, is plotted versus flow path length.

Regarding a quick and reliable input data handling, the meridional contours as well as the blade geometry are described by analytical functions, thus avoiding a time consuming point by point generation [14]. This approach reduces the necessary input data set for the overall design procedure to only 16 geometrical parameters (see Table 1) that are used for a successive variation of the complex impeller geometry.

The influence of the various parameters listed in Table 1 on the impeller geometry is illustrated in Fig. 2. Figure 3 shows three different types of impellers generated and analyzed by the design procedure described. Obviously, the input data set is easy to handle and nevertheless capable of creating a variety of impeller types which is most advantageous to the iterative design process. The blade geometry generated meets the requirements of today's numerically controlled five axis milling machines. The blade surfaces are always provided in such a way that flank milling is appropriate. Additionally, the use of analytical functions for generating the blade geometry ensures continuous partial derivatives up to the second order, which are required for the succeeding aerodynamic calculation method.

Figure 2 additionally illustrates the location of the splitter blade leading edge, which can be shifted in the axial direction, thus ensuring a sufficient blade loading control ahead of the splitter blade. Presently, the geometrical concept applied

Table 1 Geometrical input data set

Parameter	Description
r_2	impeller tip radius
r_{1i}	leading edge hub radius
r_{1t}	leading edge shroud radius
b_{2s}	exit width
l	impeller length
Δr_2	hub contour parameter
γ_N	hub exit parameter $\gamma_N = 0 \rightarrow$ radial, $\gamma_N \neq 0 \rightarrow$ diagonal
α	shroud contour parameter
γ_G	shroud exit parameter, $\gamma_G = 0 \rightarrow$ radial, $\gamma_G \neq 0 \rightarrow$ diagonal
β_{1t}	leading edge blade angle
β_{1sa}	angle for influencing backsweep
β_{2a}	blade exit angle
h	blade curvature parameter
Z_R	blade number
Z_{split}	splitter blade location
l_{indu}	inducer length

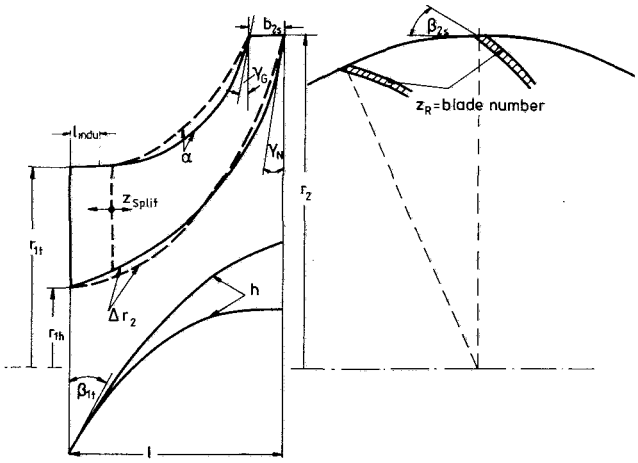

Fig. 2 Influence of the geometrical parameters on the impeller geometry

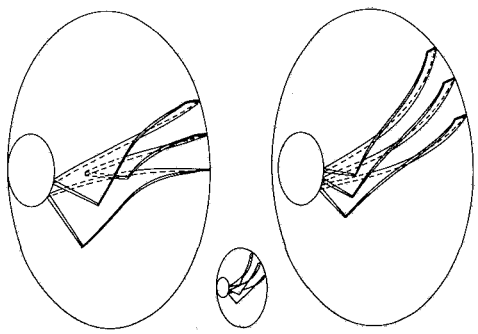

Fig. 3 Examples for impeller types generated and analyzed by the design procedure

Nomenclature

B = streamsheet thickness (hub-to-shroud)
b = streamsheet thickness (blade-to-blade)
c_f = skin friction coefficient
c_{mL} = component of meridional velocity perpendicular to laser beam axis
h_t = total enthalpy
k = ratio of specific heats
M = Mach number
$\dot{m}$ = mass flow rate
N_s = specific speed
$\mathbf{n}$ = normal unit vector of streamsurface
PS = pressure side
p = pressure
R = gas constant
r = radial coordinate
SS = suction side
s = entropy
T = temperature
u = circumferential velocity
$\mathbf{w}$ = relative velocity vector
x/s_m = dimensionless meridional shroud length
y/t = dimensionless blade pitch
z = axial coordinate
z/b = dimensionless meridional channel depth
Θ = circumferential coordinate
π_t = total pressure ratio
ψ = streamfunction
ω = angular velocity

Subscripts

0 = ambient condition
1 = impeller inlet
2 = impeller exit
m = meridional
rel = relative
t = total

assumes that the splitter geometry is the same as the main blade geometry and that the splitter is located midpitch between the main blades. Furthermore, the blade leading edges are assumed to coincide with lines of constant, z. However, if required, these assumptions may be changed.

Basic Aerodynamic Equations

The following basic flow equations are to be solved for the quasi-three-dimensional approach

Continuity:

$$\nabla \cdot (\rho \cdot \mathbf{w}) = 0 \tag{1}$$

Motion:

$$-\mathbf{w} x (\nabla x \mathbf{w}) + 2\omega x \mathbf{w} = -\nabla h_{t,\mathrm{rel}} + T\nabla s \tag{2}$$

Energy (no preswirl):

$$\nabla h_{t,\mathrm{rel}} = 0 \tag{3}$$

State of gas:

$$\rho/\rho_0 = (T/T_0)^{1/(k-1)} \cdot e^{-(s-s_0)/R} \tag{4}$$

Geometric conditions:

$$\mathbf{n} \cdot \mathbf{w} = 0 \tag{5}$$

If a streamfunction, ψ, is introduced into equations (1-5), two governing nonlinear partial differential equations of the second order are obtained describing the flow development on blade-to-blade and hub-to-shroud streamsurfaces:

Blade-to-Blade Calculation

$$A(z,\Theta)\frac{\partial^2\psi}{\partial z^2} + B(z,\Theta)\frac{\partial^2\psi}{\partial z \partial \Theta} + C(z,\Theta)\frac{\partial^2\psi}{\partial \Theta^2} + D(z,\Theta,\rho,b)\frac{\partial\psi}{\partial z} + E(z,\Theta,\rho,b)\frac{\partial\psi}{\partial\Theta} + F(z,\Theta,\rho,b,\omega,s,\partial\psi/\partial\Theta) = 0 \tag{6}$$

Hub-to-Shroud-Calculation

$$A(r,z)\frac{\partial^2\psi}{\partial r^2} + B(r,z)\frac{\partial^2\psi}{\partial r \partial z} + C(r,z)\frac{\partial^2\psi}{\partial z^2} + D(r,z,\rho,B)\frac{\partial\psi}{\partial r} + E(r,z,\rho,B)\frac{\partial\psi}{\partial z} + F(r,z,\rho,B,\omega,s,\partial\psi/\partial r) = 0 \tag{7}$$

Condition for Elliptic Equation

$$\delta = A \cdot C = (B/2)^2 > 0 \tag{8}$$

As indicated by equation (3), the aerodynamic calculation presently is limited to flows without inlet swirl although the incorporation of this effect principally is possible [15]. The condition for elliptic partial differential equations (8) is satisfied by both the blade-to-blade and hub-to-shroud equations which basically restricts the aerodynamic calculation to subsonic flows. This is a severe restriction with respect to high pressure ratio centrifugal impellers ($\pi_{t12} > 6$) which are operating with supersonic inlet conditions. For such impellers the calculation method presented momentary is only applicable if a normal shock is assumed at the tip of the impeller leading edge. With this assumption, the design procedure has been applied for a backswept impeller of pressure ratio $\pi_{t12} = 11$. Reasonable results were obtained; a comparison with measured flow field data, however, couldn't be carried out, since such data are not yet available.

A comprehensive derivative of equations (1-8) and detailed information about the numerical solution procedure are given in [9, 15]. The coefficients A – F in equations (6) and (7) are

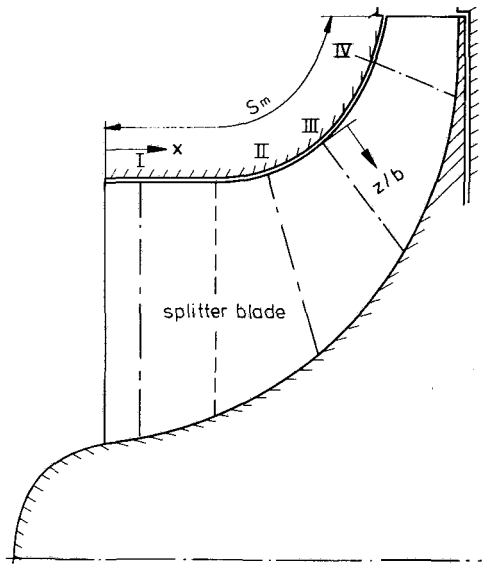

Fig. 4 Arrangement of optical measurement planes within the impeller

Table 2 Positions of laser measurement planes within the impeller [1]

Measurement plane	Location x/s_m
I	0.08
II	0.43
III	0.59
IV	0.87

functions of the impeller geometry indicated by the cylindrical coordinates, r, z and Θ. A fast and exact determination of these quantities is necessary for a satisfactory numerical solution process. However, the numerical reduction is very complex since these coefficients are complicated functions of the first and second streamsurface derivatives [15]. Therefore, it is most advantageous to describe the stream surface by a continuous mathematical function. This procedure considerably simplifies a fast and exact determination of the coefficients A – F. Primarily the hub-to-shroud surface, which for advanced centrifugal impellers usually is twisted and completely three dimensional, should be created in this way. The analytic surface generated by the 16 geometrical input parameters meets these requirements. Thus the goemetrical concept introduced simultaneously takes care of numerical, manufacturing and aerodynamic aspects. Nevertheless it should be noted that the design procedure described is restricted to impeller types compatible with the geometrical background concept. But, if required, a prescribed advanced impeller geometry can be approximated by the geometrical input parameters listed in Table 1. Such an approximation had to be carried out when the design procedure was checked with measured data.

Comparisons of Theoretical and Experimental Results

The design procedure was primarily proved with laser measurements taken within a radial discharge impeller running at 300 m/s tip speed that has 28 blades in total and 14 splitter blades. Details of the impeller geometry and of the experimental flow field analysis within this type of impeller are presented in [1]. Figure 4 illustrates the arrangement of the optical measurement planes from the inducer inlet to the impeller exit. All measurement planes are perpendicular to the shroud contour, and their correct position is submitted in Table 2.

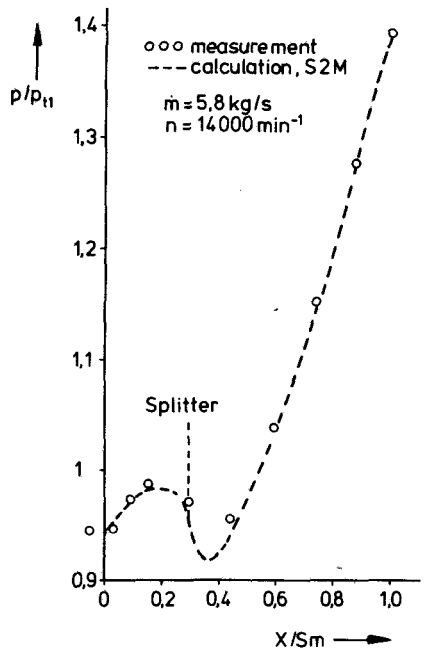

Fig. 5 Comparison of measured and calculated shroud statics: n = 14,000 min^{-1}, $\dot{m}$ = 5.8 kg/s

At first, Fig. 5 shows a comparison between calculated and measured static pressures taken along the shroud contour. Obviously an excellent agreement is obtained primarily in that area where the flow is turned to the radial direction ($x/s_m > 0.4$). This is predominantly due to the centrifugal forces which isentropically generate about 75 percent of the static pressure rise within an ordinary centrifugal impeller ($w_2/w_1 \cong 0.7$). Consequently, the comparison of calculated and measured shroud statics usually will result in a fairly good agreement which nevertheless gives only little information about the quality of the relative flow prediction. More evidence, however, is obtained by a detailed quantitative comparison with laser measurements taken within the rotating system since this approach excludes the dominating influence of the centrifugal forces. In addition, such a comparison is not only limited to the shroud region but can also be carried out within the entire flow channel.

Figure 6 shows such a comparison for measurement plane I (Fig. 4). The calculated and measured meridional velocities, referred to the rotor tip speed, are plotted against the dimensionless blade pitch for five different meridional positions (z/b = 0.1, 0.3, 0.5, 0.7, 0.9). Measurements have been carried out by means of an advanced, automated laser velocimeter [16]. The theoretical results are interpolated data taken from ten blade-to-blade solutions which were connected with the hub-to-shroud solution (Fig. 1). A pronounced boundary layer shape doesn't occur because detailed wall friction effects are neglected in this part of the aerodynamic calculation method (equations (2) and (6)).

Effects of the blade-to-blade solutions on the hub-to-shroud solution have been neglected. In spite of that, the measured data throughout properly fit the theoretical results obtained. This is mainly due to the blade-congruous flow observed in this area [1] which doesn't claim for an additional interaction between both types of stream surfaces, if the initial hub-to-shroud surface is chosen blade-congruent. Towards the impeller exit, of course, this surface deviates from the blade geometry thus taking care of slip effects.

Figure 7 shows a comparison between measurement and calculation for plane II (Fig. 4). Since plane II is located aft of the splitter blade leading edge, measurements as well as

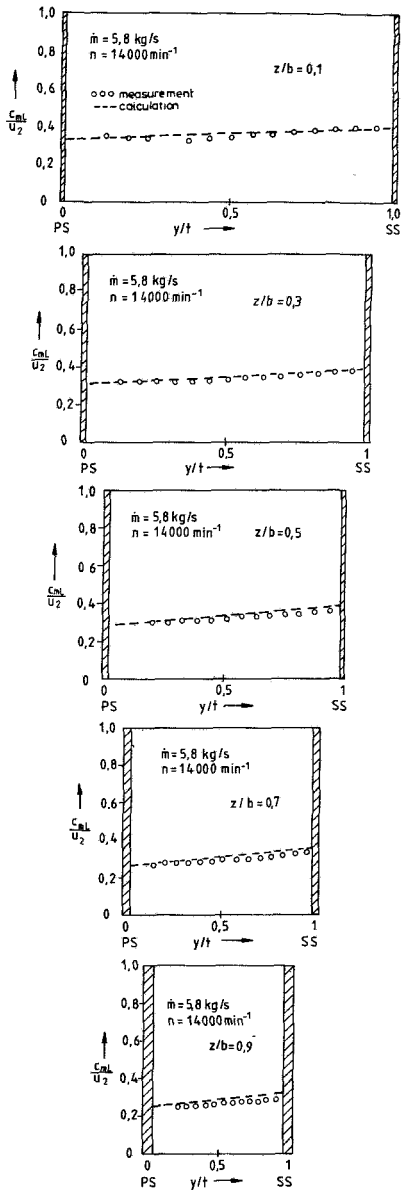

Fig. 6 Comparison of theoretical data with laser measurements at measurement plane I: n = 14,000 min^{-1}, $\dot{m}$ = 5.8 kg/s

calculations have been carried out within adjacent channels. The two channels shown are divided by the splitter blade. Again the measured data are confirmed by the theoretical results. A good agreement is obtained for all meridional positions (z/b = 0.1–0.9) and within both channels.

Figure 8 shows a similar comparison for plane III. Noticeable deviations between measured and calculated data are only observed within the shroud area of the right flow channel (z/b = 0.1), whereas in the remaining part measurements are properly fitted by the theoretical data. But even in the shroud area of the right channel, where the flow obviously tends towards a premature separation, the blade-to-blade solution reveals the correct results at the middle of the flow channel.

Measured and calculated meridional velocities of plane IV are compared to each other in Fig. 9. Significant deviations are observed in the shroud area (z/b = 0.1–0.3) within both channels where the actual flow now reveals a pronounced wake character. This deviation was to be expected since the

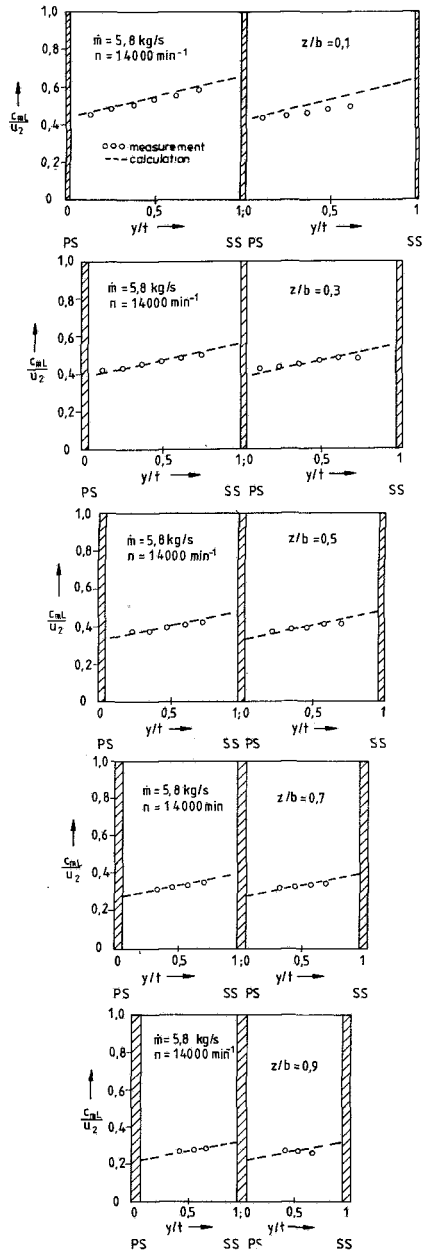

Fig. 7 Comparison of theoretical data with laser measurements at measurement plane II: $n = 14{,}000\ \text{min}^{-1}$, $\dot{m} = 5.8$ kg/s

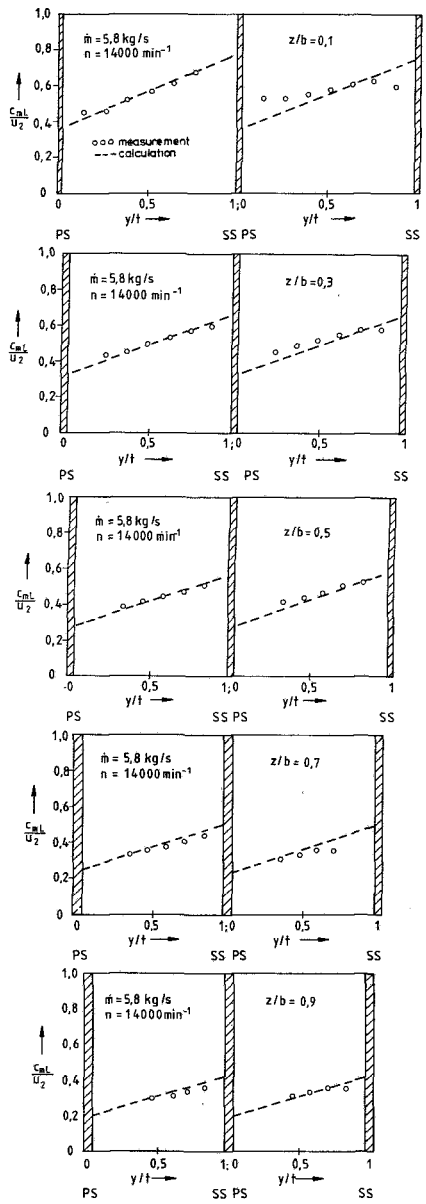

Fig. 8 Comparison of theoretical data with laser measurements at measurement plane III: $n = 14{,}000\ \text{min}^{-1}$, $\dot{m} = 5.8$ kg/s

theoretical model applied doesn't take care of detailed skin friction effects (equation (2)). Only a global entropy rise derived by assuming a constant polytropic impeller efficiency is taken into account. But even close to the impeller exit this simplified assumption is appropriate to achieve a fairly good agreement between measured and calculated data, at least in the hub region ($z/b = 0.7$–0.9). At midchannel ($z/b = 0.5$) measured data are slightly higher than the calculated which is certainly due to the wake area's displacement effect that has not been taken into account in the calculation.

Thus, the quasi-three-dimensional approach expectantly fails to predict the correct wake shape, whereas otherwise it results in a good agreement with measured data within the predominantly unseparated area. Above all, the designer of centrifugal impellers is interested in unseparated impellers, and therefore the correct prediction of a wake area's shape will not necessarily attract his utmost attention. Rather a simple but reliable information whether separation has to be expected or not is important. In this context, the boundary layer calculation method involved (Fig. 1) is believed to be a useful design tool. Figure 10 shows the result of a boundary layer calculation carried out along the shroud. The calculated local skin friction coefficient, c_f, is plotted against the dimensionless meridional length. Separation is to be expected if c_f tends toward zero. According to the results obtained separation occurs at $x/s_m \cong 0.78$ which qualitatively corresponds with the measurements. For this analysis the mean relative velocities along the shroud contour obtained by the hub-to-shroud solution have been taken as input data for the boundary layer calculations.

Design Procedure's Application

The comparison between calculated and measured data of a radially ending impeller resulted in a predominantly good agreement. In order to prove the procedure's capability for the design of advanced backswept rotors, similar comparisons

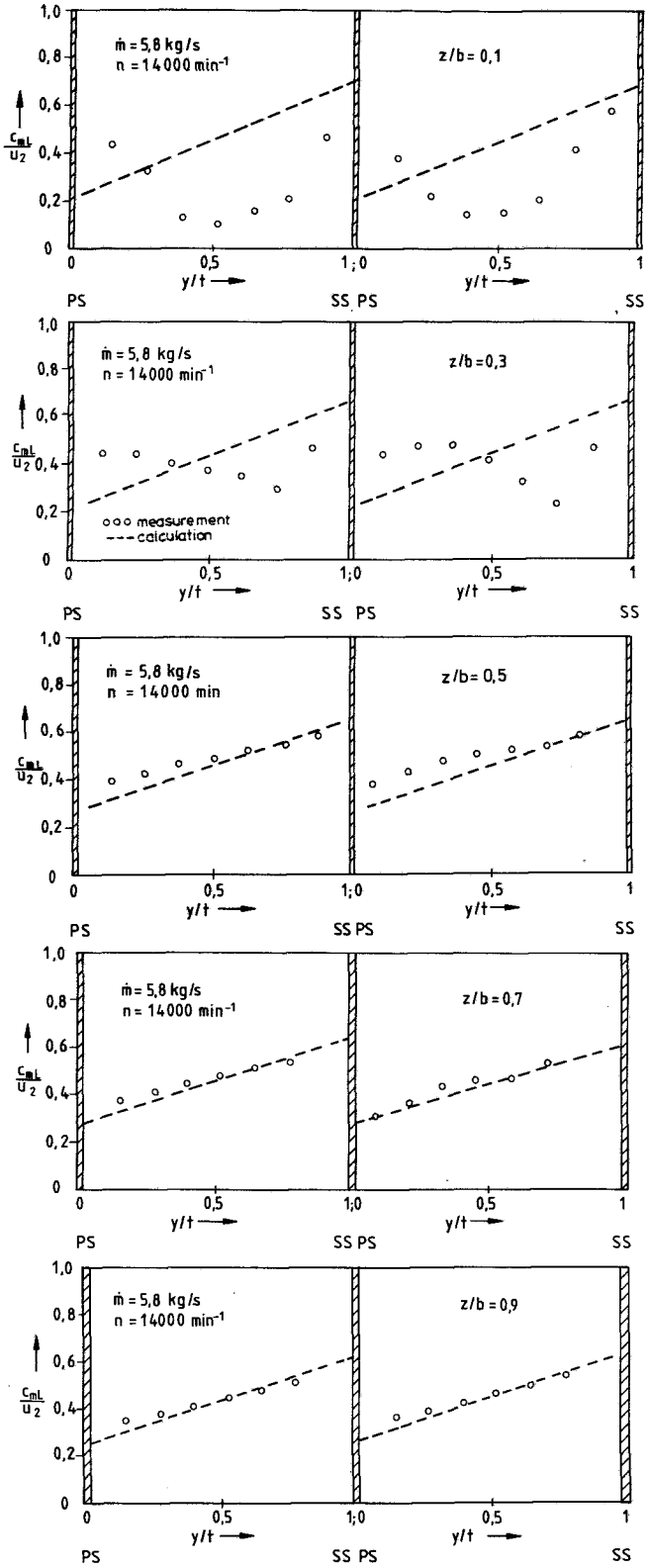

Fig. 9 Comparison of theoretical data with laser measurements at measurement plane IV: n = 14,000 min^{-1}, $\dot{m}$ = 5.8 kg/s

between theory and measurements are planned for this type of machine. The design package has been used for the design of two different types of backward leaning rotors adapted to the conditions of the DFVLR test rigs. A low specific-speed, 30-deg backswept impeller (N_s = 80) and a high specific-speed, 30-deg backswept small turbocharger impeller (N_s = 115,

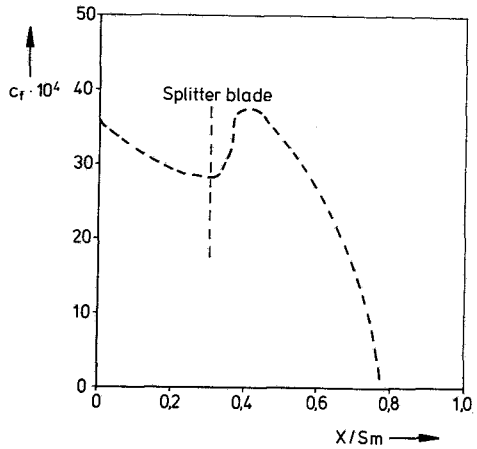

Fig. 10 Development of the local skinfriction coefficient along the shroud contour: n = 14,000 min^{-1}, $\dot{m}$ = 5.8 kg/s

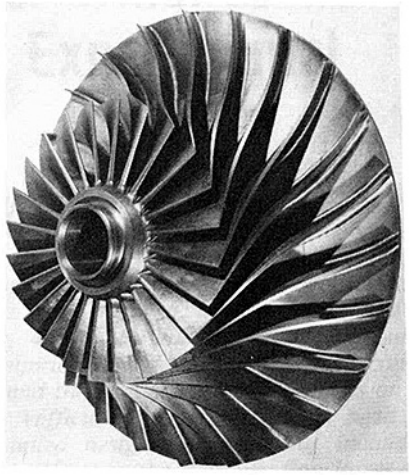

Fig. 11 Newly designed low specific speed 30-deg backswept impeller

Fig. 3) have been designed. Figure 11 shows a photograph of the low specific-speed rotor. The flow field within both types of impellers will be experimentally analyzed within the near future, thus giving additional evidence on the design procedure's reliability and applicability.

Conclusions

A computer-aided design method for centrifugal impellers has been developed with particular respect to a quick and easy input/output handling. Based on a geometrical concept, describing the impeller geometry by analytical functions a coherent design procedure is obtained that simultaneously takes care of numerical, manufacturing and aerodynamic aspects. Detailed comparisons between calculated data and laser measurements taken within a radially ending impeller resulted in a predominantly good agreement. A boundary layer calculation method involved indicated the onset of the separation and wake area. Thus the design procedure developed obviously is a useful design tool with regard to a reliable relative flow field prediction and may be used to reduce the wake area's size.

References

1 Krain, H., "A Study on Centrifugal Impeller and Diffuser Flow," ASME JOURNAL OF ENGINEERING FOR POWER, Vol. 103, No. 4, Oct. 1981, pp. 688-697.

2 Johnson, M. W., and Moore, J., "Secondary Flow Mixing Losses in a Centrifugal Impeller," ASME Paper No. 82-GT-44.

3 Runstadler, P. W., Jr., Dolan, F. X., and Dean, R. C. Jr., *Diffuser Data Book*, Creare, TN-186, 1975, p. 88.

4 Krain, H., "Experimental and Theoretical Investigation on the Fluid

Dynamics of a Centrifugal Compressor Stage," *Proceedings of the CASI Centrifugal Compressor Symposium*, Toronto, May 1982, p. 33.

5 Waitman, B. A., Reneau, L. R., and Kline, S. J., "Effects of Inlet Conditions on Performance of Two-Dimensional Subsonic Diffusers," ASME *Journal of Basic Engineering*, Sept. 1961, pp. 349–360.

6 Hirsch, Ch., and Warzee, G., "A Finite Element Method for Through-Flow Calculations in Turbomachines," ASME Paper No. 76-FE-12.

7 Howard, J. H. G., and Osborne, C., "A Centrifugal Compressor Flow Analysis Employing a Jet-Wake Passage Flow Model," ASME *Journal of Fluids Engineering*, 1977, pp. 141–147.

8 Bosman, C., and El-Shaarawi, M. A. I., "Quasi-Three-Dimensional Numerical Solution of Flow in Turbomachines," ASME *Journal of Fluids Engineering*, Vol. 99, 1977, pp. 132–140.

9 Krain, H., and Eckard, D., "The Flow Field in a High-Speed Centrifugal Impeller: A Comparison of Experimental and Theoretical Results," *Proceedings of the First International Conference on Centrifugal Compressor Technology*, Madras, Feb. 1978, B1-25.

10 Moore, J., and Moore, J. G., "Calculations of Three-Dimensional, Viscous Flow and Wake Development in a Centrifugal Impeller," in *Performance Prediction of Centrifugal Pumps and Compressors*, 1980, pp. 61–67.

11 Walitt, L., "Numerical Analysis of the Three Dimensional Viscous Flow Field in a Centrifugal Impeller," AGARD-CP-282, 1980, p. 28.

12 Wu, C. H., " A General Theory of Three-Dimensional Flow in Subsonic and Supersonic Turbomachines of Axial, Radial and Mixed-Flow Types," NACA TN-2604, 1952, p. 92.

13 Bradshaw, P., and Unsworth, K., "An Improved Fortran Program for the Bradshaw-Ferriss-Atwell Method of Calculating Turbulent Shear Layers," I. C. Aero Report 74-02, Feb. 1974, p. 51.

14 Casey, M. V., "A Computational Geometry for the Blades and Internal Flow Channels of Centrifugal Compressors," ASME Paper No. 82-GT-155, p. 10.

15 Krain, H. "Contribution to the Quasi-Three-Dimensional Calculation Within Centrifugal Compressor Impellers," (in German), Doctoral thesis, Technische Hochschule Aachen, Dec. 1975, p. 185.

16 Schodl, R., "A Laser-Two-Focus (L2F) Velocimeter for Automatic Flow Vector Measurements in the Rotating Components of Turbomachines," ASME Paper No. 1980, In *Measurement Methods in Rotating Components of Turbomachinery*, pp. 139–147.

17 Rodgers, C., "The Performance of Centrifugal Compressor Channel Diffusers," ASME Paper No. 82-GT-10, p. 13.